

Tanshinone IIA alleviates the damage of neurocytes by targeting GLUT1 in ischaemia reperfusion model (*in vivo* and *in vitro* experiments)

Xinxing Wang^{1*}, Jing Wang^{1*}, Xiangyang Wang¹, Yang Wang², Haibo Tong¹

¹Department of Neurosurgery, Shanxi Bethune Hospital, Shanxi Academy of Medical Science, Third Hospital of Shanxi Medical University, Shanxi, China, ²Department of Otolaryngology Head and Neck Surgery, First Hospital of Shanxi Medical University, Shanxi, China

*Xinxing Wang and Jing Wang contributed equally to this study and were the co-first authors of this study.

Folia Neuropathol 2020; 58 (2): 176-193

DOI: <https://doi.org/10.5114/fn.2020.96983>

Abstract

Stroke is partial or complete brain dysfunction combined with acute cerebral circulatory disorders, and it affects millions of individuals around the world each year. A total of 70-80% of patients experience ischaemic stroke caused by disturbances in cerebral circulation, leading to cerebral ischaemia, neuronal apoptosis, and necrosis. Tanshinone IIA is a natural compound extracted from *Salvia miltiorrhiza* and has been proven to assist in recovery from cerebral ischaemia reperfusion injury. GLUT1 is ubiquitously expressed in all types of tissues in the human body and has important physiological functions due to its glucose uptake ability. This experiment was performed to detect the effect of GLUT1 in promoting the therapeutic effect of tanshinone IIA. Here, we found that tanshinone IIA treatment increased the viability of neurons and promoted the recovery of brain function, and that the concentration of glucose in serum and cultured medium was also increased. We noticed that these effects might be mediated by an increased glucose uptake ability. In addition, we further found that the PI3K/mTOR/HER3 signalling pathway played an important role in regulating these effects. Thus, we thought that overexpression of GLUT1 might be an important target in the treatment of cerebral ischaemia-reperfusion.

Key words: tanshinone IIA, GLUT1, ischaemia reperfusion, PI3K/mTOR signalling pathway, mitochondrial function.

Introduction

Cerebral ischaemia-reperfusion (I/R) is one of the major health problems around the world. It often causes irreversible damage to brain tissues and leads to functional impairment and the death of neurons [1,39]. Previous studies have shown that approximately 10% of patients suffer from pre-stroke dementia, 10% suffer from post-stroke dementia after their first stroke, and more than 30% of patients suffer from dementia after recurrent strokes [26,35].

However, the treatments of I/R are still limited. Tanshinone IIA is a fat-soluble component of *Salvia miltiorrhiza*. A previous study found that tanshinone IIA increased the blood flow in the heart and improved myocardial metabolic disorders by improving the tolerance of cardiomyocytes to hypoxia [46]. In addition, tanshinone IIA also reduced the area of infarction, improved myocardial contractility, and promoted myocardial regeneration [9]; it has also been considered as a treatment for cardiovascular events

Communicating author

Haibo Tong, Department of Neurosurgery, Shanxi Bethune Hospital Shanxi Academy of Medical Science, No. 99 Longcheng Road, Shanxi, China, 030032, e-mail: wangxinxindoc@163.com

[13]. GLUT1 was first identified in a foetal skeletal muscle cell line by using a cDNA probe [23] and is commonly regarded as the “neuronal glucose transporter” [32]. Recently, a study showed that GLUT1 has important functions in cell processes [27,30]. Thus, we speculated that overexpression of GLUT1 might enhance the therapeutic effect of tanshinone IIA for the treatment of middle cerebral artery occlusion (MCAO). In this study, we found that tanshinone IIA could increase the viability of neurons and help recover the function of the mouse brain. It increased the concentration of glucose in serum samples of mice and culture medium from cells, and we further noticed that these effects might be mediated by an increase in glucose uptake ability. In addition, we found that increased activation of the PI3K/mTOR/HER-3 signalling pathway played an important role in the regulation of these effects, and overexpression of GLUT1 enhanced the effect of tanshinone IIA. We thought that GLUT1 might be a therapeutic target for cerebral ischaemia-reperfusion.

Material and methods

Ethical statement

This study was carried out in strict accordance with the recommendations in the Guide for the Care and Use of Laboratory Animals of the National Institutes of Health (USA). All experiments were conducted in accordance with the Declaration of Helsinki and were approved by the Ethics Committee of the Shanxi Bethune Hospital Shanxi Academy of Medical Science.

Animal model and grouping

6-8-week-old GLUT1 knockdown mice, GLUT1 overexpression mice and C57BL mice were purchased from Cyagen Biosciences Company (No. SCXK2016-0002). The 10 C57BL mice, five GLUT1 knockdown mice, and five GLUT1 overexpression mice were housed at 25°C under a 12-h light-dark cycle with food and water freely available. The mice were then divided into four groups: operation group (NC), tanshinone IIA treatment group (TT), tanshinone IIA treatment combined with GLUT1 overexpression group (TO), and tanshinone IIA treatment combined with GLUT1 inhibition group (TI). The mice were first anaesthetised with 100 mg/kg ketamine and 10 mg/kg xylazine and placed on a stereotaxic device. Then, the middle cerebral artery (MCA) was

exposed and occluded with a soldering iron placed directly on the dura [16]. After surgery, the soft tissues were replaced and the skin was closed using 5-0 nylon suture. Buprenorphine was used to prevent post-operative pain and was given every 6 h at a dose of 0.3 mg/kg. After the model was constructed in mice, the mice were treated with 15 mg/kg tanshinone IIA (T4952, Sigma) for seven days through tail intravenous injection, and the mice in the sham group received the same volume of normal saline through tail intravenous injection ($n = 5$).

Morris water maze test

The Morris water maze (MWM) test was performed in order to evaluate the spatial learning and memory ability of the mice and was performed according to previous protocols [42]. All of the experimental steps were performed in a quiet environment. The swimming pool used was a circular tank (diameter: 122 cm, divided into four quadrants). The water temperature was kept at approximately 20°C. A 10 cm² hidden circular platform was located in the quadrant of NE, and spatial acquisition trials were performed on five continuous days with four trials on each day, starting in the SE, S, NW, and W (Table I). If the mice were unable to reach the platform in 1 min, the mice were guided to the platform. Before performing the following experiments, the mice were kept on the platform for 15 s. Escape latency was set as the time the mice used to reach the escape platform, and the escape test was performed on the sixth day. The time travel distance that mice spent in the target quadrant and the number of times the mice crossed the zone was recorded after removing the escape platform and the mice swam for 60 s. All of the steps were monitored using image detectors and analysed using the ANY-maze software (ANY-maze). After the MWM test, brain tissues and serum samples of mice were collected to perform the following experiments.

Table I. Starting positions for the spatial and probe tests of Morris water maze

Day	Trial 1	Trial 2	Trial 3	Trial 4
1	S	W	NW	SE
2	NW	S	SE	W
3	SE	NW	W	S
4	W	SE	S	NW
5	S	NW	W	SE

NW – Northwest, S – South, SE – Southeast, W – West.

TTC staining

After brain tissue was collected, tissues were stored at -20°C for 30 min. Then the tissues were cut into 2 mm slices and stained with 2% TTC solution for 30 min at 37°C away from light. After washing with phosphate-buffered saline (PBS), images of the slices were acquired.

Vector construction

Full-length GLUT1 cDNA was cloned using a polymerase chain reaction (PCR) method with the following primers: Forward: 5'-GGGAGCTAACATCTCCAAGTCT-3', Reverse: 5'-CTGGCATCAACGCTGTCTTC-3'. The PCR product of GLUT1 and pCDNA3.1-3×Flag was digested with BamHI (R3136S, NEB) and XhoI (R0146S, NEB), and then the PCR product and the digested vector was linked to construct the pCDNA3.1-3×Flag-GLUT1 overexpression vector. Then, the GLUT1 overexpression vector was transfected into Neuro-2a cells using Lipo 3000 transfection reagent (L3000015, Thermo) for 48 h, and the stable expressing cells were screened using G418 (11811031, Thermo). The GLUT1 knockdown vector was constructed as described in a previous study [48]. The pair of oligos were acquired using the following primers: Forward: 5'-CACCGTCTCTTCAGATGTGCCGTT-3', Reverse: 5'-AAACAACGGCACATCTGAAAGAGAC-3'. The CRISPR vector and the pair of oligos were digested with BsmBI (R0580S, NEB) at 37°C for 30 min. The oligos were phosphorylated with T4 PNK (M0202S, NEB) and incubated at 37°C for 30 min followed by incubation at 95°C for 5 min. The digested vector and oligos were linked with Quick Ligase and then transfected into 293T cells to construct the GLUT1-knockdown lentiviral vector. The stably expressed cells were screened using $2\ \mu\text{g}/\text{ml}$ puromycin (A1113802, Thermo).

Cell culture and grouping

Neuro-2a cells were purchased from ATCC (CCL-131). The cells were cultured in Dulbecco's modified Eagle's medium (11995065, Thermo) supplemented with 10% foetal bovine serum (FBS, 16140071, Thermo) at 37°C and humidified in a 5% CO_2 atmosphere. Then, the cells were divided into four groups: the normal group (NC), tanshinone IIA treatment group (TT), tanshinone IIA treatment combined with GLUT1 overexpression group (TO), and the tanshi-

none IIA treatment combined with GLUT1 inhibition group (TI). Before performing the following experiments, cells in the tanshinone IIA treatment group were treated with $1\ \mu\text{M}$ tanshinone IIA for 1 h.

Glucose uptake assays

Glucose uptake assays were performed according to the manufacturer's protocol (ab136955, Abcam). Cells and brain tissues were lysed with extraction buffer, and then the samples were incubated with neutralising buffer and assay buffer. Then, the samples and standard were incubated with reaction buffer A for 1 h at 37°C followed by incubation with extraction buffer for 40 min at 90°C . After cooling on ice and incubating with reaction buffer B, the absorbance value at 412 nm was measured using a microplate reader (Multiskan FC, Thermo).

Measurement of cellular and serum glucose concentration

Measurement of the glucose concentration in the cells and brain tissues was performed according to the manufacturer's protocol (ab65333, Abcam). Briefly, cells and brain tissues were first lysed with assay buffer. After the samples were added into each well, they were mixed with reaction buffer and incubated at 37°C for 30 min. The absorbance value at 570 nm was measured using a microplate reader (Multiskan FC, Thermo).

MTT assay

Cells were first seeded into a 96-well plate at a concentration of $1 \times 10^5/\text{well}$. The cells were grouped and treated as previously described. Then, the cells were incubated with MTT reagent (M6494, Thermo) at a final concentration of 5 mg/ml. After incubation with MTT for 4 h, the cells were incubated with $150\ \mu\text{l}$ DMSO for 10 min at room temperature with gentle shaking. The absorbance value at 570 nm was measured using a microplate reader (Multiskan FC, Thermo). The viability rate was calculated using the following equation: $\text{viability rate} = [1 - (\text{Absorbance value}_{\text{Experiment}} - \text{Absorbance value}_{\text{Blank}}) / (\text{Absorbance value}_{\text{NC}} - \text{Absorbance value}_{\text{Blank}})] \times 100\%$.

RNA extraction

RNA extraction was performed according to the protocol of the total RNA extraction kit (R1200,

Solarbio). Briefly, cells and mice were divided into four groups as previously described, and then cells and brain tissues were lysed with lysis buffer and incubated at room temperature for 5 min. After that, the lysates were incubated with chloroform, and the water phase was collected in an absorption tube. After washing with washing buffer, the RNA was eluted using elution buffer. The concentration of the RNA was determined using a NanoDrop Lite (Thermo). The RNA was stored at -80°C until performing the following experiments.

Reverse transcription and real-time quantitative polymerase chain reaction

Reverse transcription and real-time quantitative polymerase chain reaction (qPCR) were performed according to the manufacturer's protocol (T2210, Solarbio). Briefly, the reaction mixture was prepared as recommended, and the primers used were as follows: COX-2: Forward: 5'-GTTTGGTCTGGTGCCTGGTT-3', Reverse: 5'-AGCACATCGCACACTCTGTTATGT-3'; IL-1 β : 5'-GGCACGTATGAGCTGAAAGCT-3', Reverse: 5'-TGCACA-AACTCATGGAGAACAC-3'; PGE2: Forward: 5'-CGGGCATCGATCGATAAGCTAC-3', Reverse: 5'-CGGCGCATGCTACGATCGACTCG-3'; MCP-1: Forward: 5'-TCTGTGCTGAC-CCCAAGCA-3', Reverse: 5'-GTCTGCATTTCTGTCCAG-GTT-3'. The PCR consisted of: reverse transcribe at 50°C for 20 min and denaturation at 95°C for 3 min, and these steps were repeated for 45 cycles: denaturation at 95°C for 15 s, annealing at 60°C for 30 s, and extend at 72°C for 60 s. Glyceraldehyde-3-phosphate dehydrogenase (GAPDH) was used as an internal control. The expression of each target gene was determined using the $2^{-\Delta\Delta C_q}$ method [29].

Western blotting analysis

Cells were divided into four groups and cultured as previously described. Then, the cells were lysed with lysis buffer (4% SDS, 10 mM IAA, 50 mM DTT, and protease inhibitor cocktail). The concentrations of the protein samples were determined using a BCA assay. Then, 60 μg of each protein sample was used to perform 10% SDS-PAGE. After electrophoresis, the proteins were transferred onto a PVDF membrane. The membranes were blocked with 5% skimmed milk and incubated with the primary anti-bodies (1:1000, anti-GLUT1 [ab115730], anti-ACO2 [ab129069], anti-Hexokinase II [ab104836], anti-LDHA [ab84716], anti-MDH2 [ab181857], anti-HIF-1 α [ab1], anti-AKT

[ab179463], anti-p-AKT [ab38449], anti-mTOR [ab2732], anti-p-mTOR [ab109268], anti-HER3 [ab32121], anti-p-HER3 [ab101407], Abcam) overnight at 4°C followed by incubation with the secondary antibody for 1 h at room temperature. The expression of each target protein was detected using a chemiluminescent immunoassay. GAPDH was used as an internal control.

ELISA

The ELISA assay was performed according to the manufacturer's protocol (Neurotrophin-3 ELISA kit [ab213882], Calprotectin ELISA kit [ab263885], GFAP ELISA kit [ab233621], ROS Assay kit [ab186029], Nitric Oxide Assay kit [ab65328], and GSH/GSSG Ratio Detection Assay kit [ab138881], Abcam). Briefly, cells and serum were added into each well of a 96-well plate and incubated at 37°C for 90 min, followed by incubation with target antibodies at 37°C for 60 min. After washing with washing buffer, samples were incubated with ABC working solution at 37°C for 30 min. Samples were incubated with TMB agent for 25 min at 37°C followed by incubation with stop solution. The absorbance value at 450 nm was measured using a microplate reader (Multiskan FC, Thermo).

Statistical analysis

The data of each experiment are presented as the mean \pm S.E.M. Each experiment was repeated three times independently. One-way ANOVA was used to analyse the differences among groups using SPSS 22.0 software. *P* value < 0.05 was set as a statistically significant difference.

Results

The expression of GLUT1 in each group of mice and cells without tanshinone IIA treatment

As shown in Figure 1A and B, the expression levels of GLUT1 in the cells and mouse model not treated with tanshinone IIA were detected using western blotting analysis. The expression level of GLUT1 in the NC, GO (GLUT1 overexpression), and GI (GLUT1 inhibition) groups of cells were 1.34 ± 0.10 , 1.71 ± 0.13 , and 0.35 ± 0.03 , respectively. The expression level of GLUT1 in the NC, GO, and GI groups of the mouse model were 0.50 ± 0.04 , 0.78 ± 0.06 , and 0.20 ± 0.02 , respectively. The area of ischaemia was significantly reduced after overexpression of GLUT1. These results indicated the

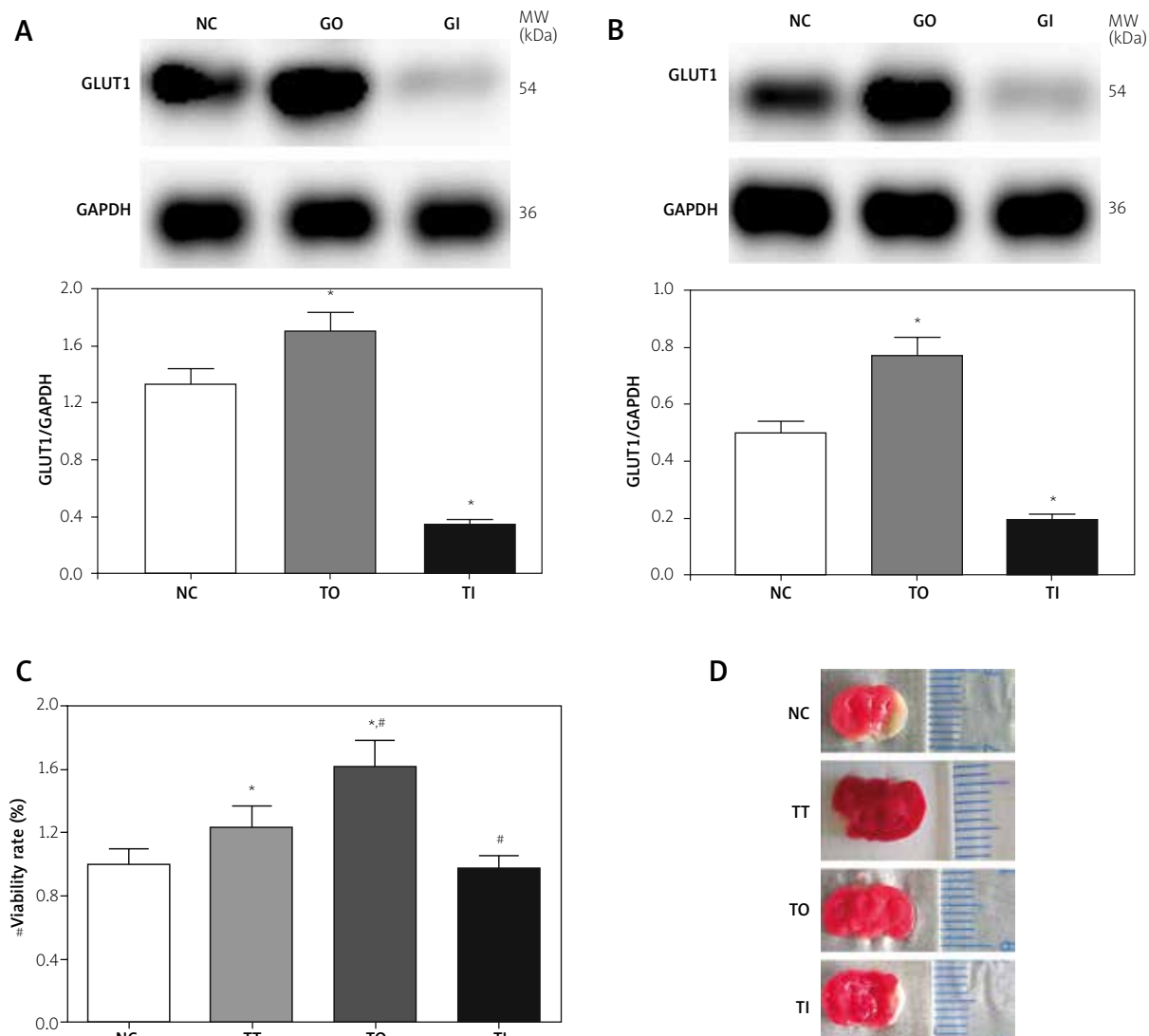


Fig. 1. Evaluation of GLUT1 overexpression and inhibition model in cell and mice. **A)** Expression of GLUT1 in cells without treatment of tanshinone IIA. **B)** Expression of GLUT1 in mice without treatment of tanshinone IIA. **C)** The viability rate of cells in NC, TT, TO, and TI groups. Data presented as mean \pm SD. Each experiment was repeated three times independently. * $p < 0.05$ compared with NC group. # $p < 0.05$ compared with TT group. GO – GLUT1 overexpression group without treatment of tanshinone IIA. GI – GLUT1 inhibition group without treatment of tanshinone IIA.

successful establishment of GLUT1 overexpression and inhibition models in cells and mice.

The effect of tanshinone IIA on cognitive performance of mice in the acquisition trial and probe test of MWM

The performance of mice on the MWM test is presented in Figure 2. The escape latency of the mice was detected for five continuous days, and the aver-

age escape times were 72.3 ± 6.2 , 68.5 ± 6.1 , 60.2 ± 5.6 , 51.3 ± 5.0 and 44.7 ± 4.2 in the NC group, 65.3 ± 6.2 , 56.2 ± 5.7 , 48.2 ± 4.1 , 41.0 ± 3.4 and 35.2 ± 3.1 in the TT group, 62.1 ± 5.5 , 51.3 ± 4.8 , 40.2 ± 3.6 , 33.5 ± 3.1 and 27.1 ± 2.5 in the TO group, and 70.2 ± 6.9 , 61.3 ± 5.9 , 52.4 ± 5.2 , 47.3 ± 4.3 and 41.0 ± 3.5 in the TI group. The average number of platform crossings in these groups were 2.8 ± 0.4 , 3.3 ± 0.6 , 4.9 ± 0.7 , and 2.9 ± 0.5 , respectively. The times spent in the target quadrant

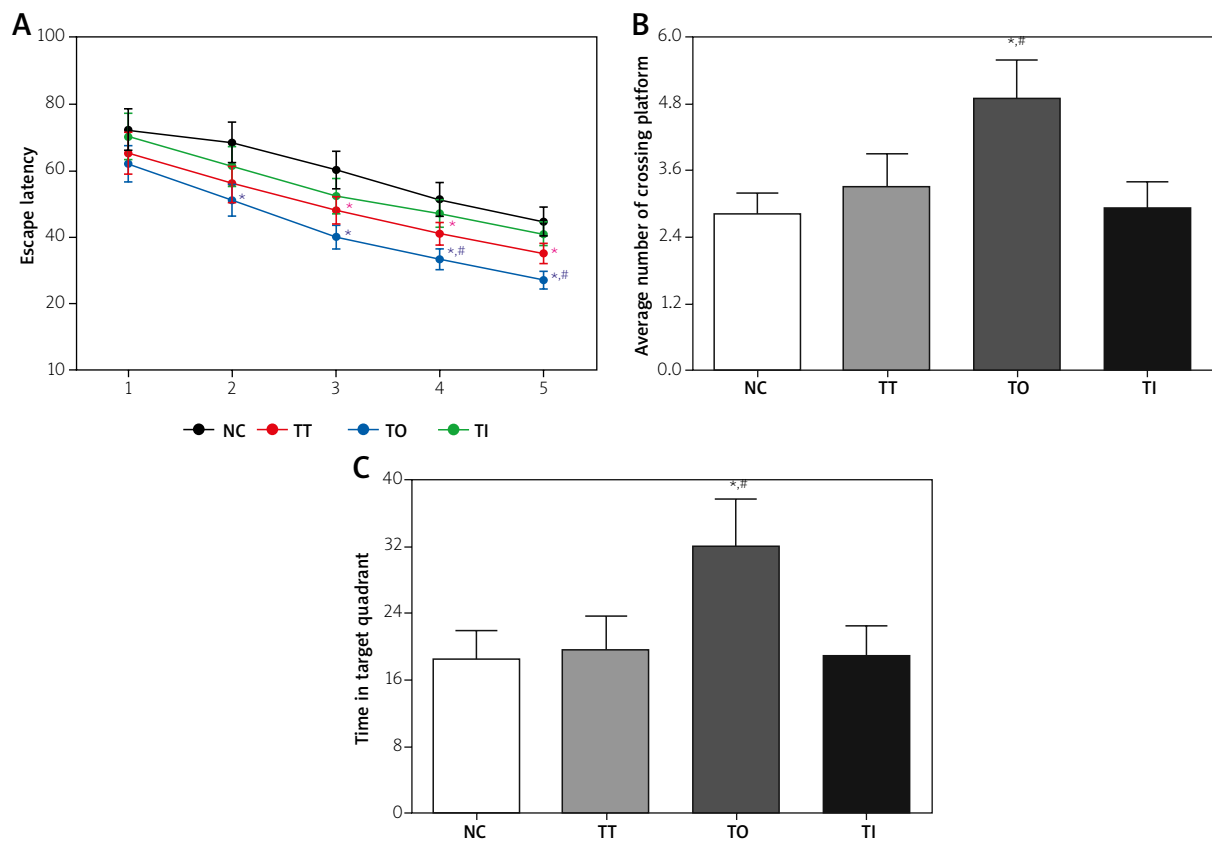


Fig. 2. Detection of memory function using MWM. **A)** The escape latency of mice in each group in 5 consecutive days. **B)** The average number of crossing platform of mice in each group. **C)** The time in target quadrant of mice in each group. Data presented as mean \pm SD. Each experiment was repeated three times independently. * $p < 0.05$ compared with NC group. # $p < 0.05$ compared with TT group.

in these groups were 18.5 ± 3.5 , 19.6 ± 4.1 , 25.1 ± 5.0 , and 18.8 ± 3.7 s, respectively. These results indicated that tanshinone IIA treatment enhanced the function of memory and that the overexpression of GLUT1 enhanced this trend.

The effect of tanshinone IIA on cellular viability

As shown in Figure 1C, the viability rate in the TT, TO, and TI groups under tanshinone IIA treatment were 123.1 ± 13.4 , 161.2 ± 17.1 , and 96.4 ± 9.1 , respectively. The viability was significantly increased in the TT and TO groups compared with the NC group ($p < 0.05$) and was significantly increased in the TO group ($p < 0.05$) and significantly decreased in the TI group ($p < 0.05$) compared with the TT group. These results indicate that overexpression of GLUT1 increased the viability rate of the cells.

The effect of tanshinone IIA on the detection of glucose concentration and glucose intake ability in the mouse and cell models

As shown in Figure 3, the relative concentration of glucose in the NC, TT, TO, and TI groups of the mouse model were 1.00 ± 0.13 , 0.85 ± 0.11 , 0.61 ± 0.07 , and 0.94 ± 0.13 , respectively. The relative concentration of glucose in the NC, TT, TO, and TI groups of the cell model were 1.00 ± 0.16 , 0.81 ± 0.12 , 0.57 ± 0.08 , and 0.99 ± 0.13 , respectively. The glucose uptake changing fold in the NC, TT, TO, and TI groups of the mouse model were 1.00 ± 0.13 , 1.31 ± 0.19 , 1.88 ± 0.27 , and 1.08 ± 0.16 , respectively. The glucose changing fold in the NC, TT, TO, and TI groups of the cell model were 1.00 ± 0.15 , 1.26 ± 0.17 , 1.74 ± 0.22 , and 1.09 ± 0.17 , respectively. These results showed that tanshinone IIA treatment decreased the concentration of glucose in the serum samples and

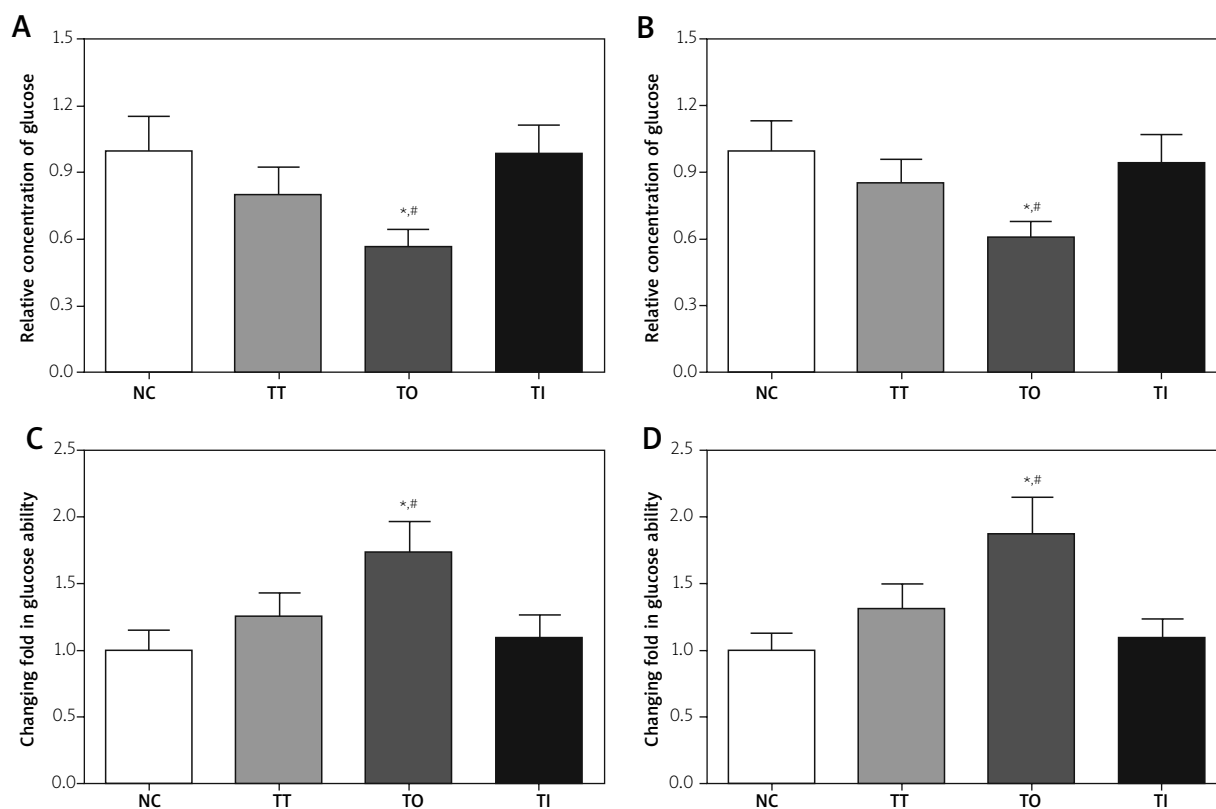


Fig. 3. Detection of glucose concentration and glucose uptake ability in cultured medium of cells and serum sample of mouse model. **A)** The relative concentration of glucose in cultured medium of cells. **B)** The relative concentration of glucose in serum sample of mouse model. **C)** The changing fold in glucose uptake ability in cells. **D)** The changing fold in glucose uptake ability in brain tissue of mouse model. Data presented as mean \pm SD. Each experiment was repeated three times independently. * $p < 0.05$ compared with NC group. # $p < 0.05$ compared with TT group.

increased the glucose uptake ability in brain tissues and cells but not significantly, but after overexpression of GLUT1, the changes became significant.

The effect of tanshinone IIA on the expression of target genes in the mouse and cell models

As shown in Figure 4, the expression level of COX-2 in the brain tissue of mice from the NC, TT, TO, and TI groups were 1.6 ± 0.2 , 1.1 ± 0.1 , 0.7 ± 0.1 , and 1.4 ± 0.2 , respectively. The expression of COX-2 was significantly decreased in the TT and TO groups ($p < 0.05$) compared with the NC group and was significantly decreased in the TO group ($p < 0.05$) compared with the TT group. The expression levels of IL-1 β in these groups were 2.1 ± 0.4 , 1.7 ± 0.3 , 1.1 ± 0.1 , and 1.9 ± 0.2 , respectively. The expression of IL-1 β was significantly

decreased in the TO group ($p < 0.05$) compared with the NC and TT groups. The expression levels of PGE2 in these groups were 1.3 ± 0.3 , 1.0 ± 0.2 , 0.6 ± 0.1 , and 1.2 ± 0.2 , respectively. The expression of PGE2 was significantly decreased in the TO group ($p < 0.05$) compared with the NC and TT groups. The expression levels of MCP-1 in these groups were 1.8 ± 0.3 , 1.3 ± 0.2 , 0.7 ± 0.1 , and 1.6 ± 0.3 , respectively. The expression of MCP-1 presented a similar trend to PGE2. As shown in Figure 5, the expression levels of COX-2 in the NC, TT, TO, and TI groups of cells were 1.3 ± 0.2 , 1.0 ± 0.2 , 0.6 ± 0.1 , and 1.2 ± 0.3 , respectively. The expression of COX-2 was significantly decreased in the TO group ($p < 0.05$) compared with the NC and TT groups. The expression levels of IL-1 β in these groups were 1.6 ± 0.3 , 1.2 ± 0.2 , 0.8 ± 0.1 , and 1.4 ± 0.3 , respectively. The expression levels of PGE2 in these groups were 1.5 ± 0.3 , 1.2 ± 0.2 , 0.7 ± 0.1 , and 1.3 ± 0.2 ,

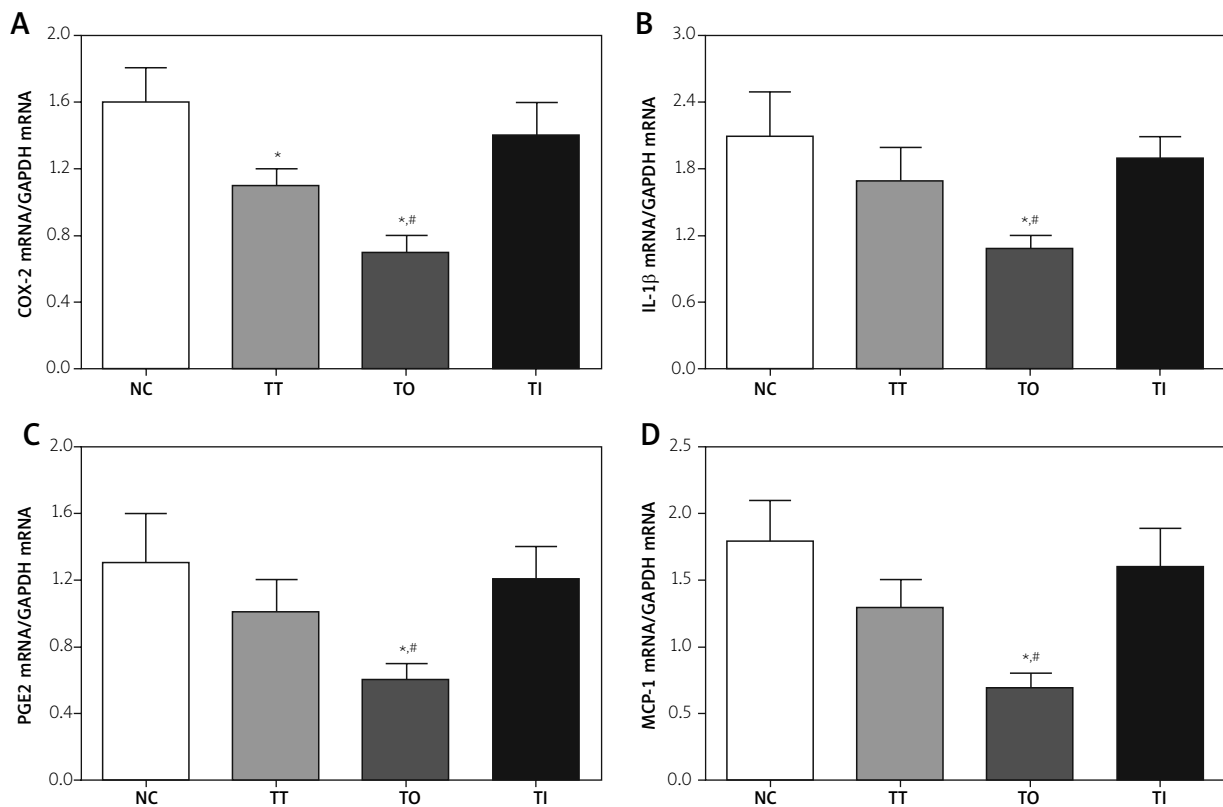


Fig. 4. The expression level of COX-2, IL-1β, PGE2, and MCP-1 in cells. **A)** The expression level of COX-2 in cells. **B)** The expression level of IL-1β in cells. **C)** The expression level of PGE2 in cells. **D)** The expression level of MCP-1 in cells. Data presented as mean ± SD. Each experiment was repeated three times independently. **p* < 0.05 compared with NC group. #*p* < 0.05 compared with TT group.

respectively. The expression levels of MCP-1 in these groups were 1.5 ± 0.3 , 1.1 ± 0.2 , 0.6 ± 0.1 , and 1.2 ± 0.2 , respectively. The expression of IL-1β, PGE2, and MCP-1 presented similar trends as COX-2.

The effect of tanshinone IIA on expression of target proteins in the mouse and cell models

As shown in Figure 6A, the expression levels of ACO2, hexokinase 2, LDHA, and MDH2 in each group of the cell model were detected using western blotting analysis. Respectively, the expression was: ACO2 0.21 ± 0.02 , 0.77 ± 0.06 , 1.22 ± 0.10 , and 0.45 ± 0.04 ; hexokinase 2 0.35 ± 0.0 , 0.82 ± 0.07 , 1.30 ± 0.11 , and 0.70 ± 0.06 ; LDHA 1.36 ± 0.11 , 1.26 ± 0.10 , 0.76 ± 0.06 , and 1.39 ± 0.12 ; and MDH2 0.50 ± 0.04 , 1.15 ± 0.10 , 1.46 ± 0.12 , and 1.04 ± 0.09 . As shown in Figure 6B, the expression levels of ACO2, hexokinase 2, LDHA, and MDH2 in each group of the mouse model were detected using western blotting analysis. Respective-

ly, the expression was: ACO2 0.01 ± 0.00 , 0.25 ± 0.02 , 0.89 ± 0.07 , and 0.41 ± 0.03 ; and hexokinase 2 0.15 ± 0.01 , 0.62 ± 0.05 , 0.86 ± 0.07 , and 0.01 ± 0.00 . These results show that the expression of aerobic oxidation of glucose-related enzymes was increased after tanshinone IIA treatment, and it was even higher after overexpression of GLUT1, indicating that tanshinone IIA activates the aerobic oxidation of glucose, and overexpression enhances this process.

The effect of tanshinone IIA on activation of the PI3K/AKT/mTOR signalling pathway in the mouse and cell models

As shown in Figure 7A, the expression of GLUT1 and HIF-1α and the ratio of p-AKT/AKT, p-mTOR/mTOR, and p-HER3/HER3 in each group of the cell model were detected using western blotting analysis. Respectively, the expression was: GLUT1 0.52 ± 0.04 , 1.38 ± 0.11 , 2.06 ± 0.17 , and 0.84 ± 0.07 ; and

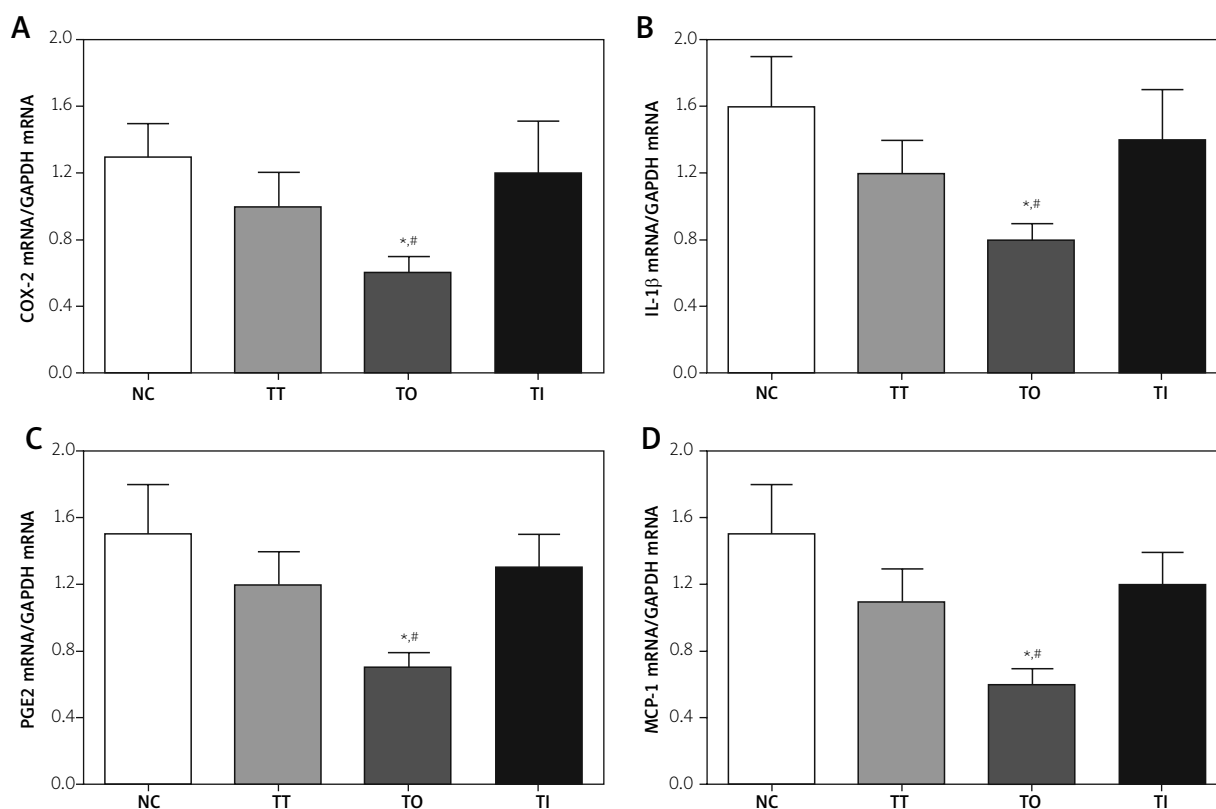


Fig. 5. The expression level of COX-2, IL-1 β , PGE2, and MCP-1 in brain tissue of mouse model. **A)** The expression level of COX-2 in brain tissue of mouse model. **B)** The expression level of IL-1 β in brain tissue of mouse model. **C)** The expression level of PGE2 in brain tissue of mouse model. **D)** The expression level of MCP-1 in brain tissue of mouse model. Data presented as mean \pm SD. Each experiment was repeated three times independently. * $p < 0.05$ compared with NC group. # $p < 0.05$ compared with TT group.

HIF-1 α 1.00 ± 0.08 , 1.02 ± 0.09 , 0.80 ± 0.07 , and 1.17 ± 0.10 . Respectively, the ratio of p-AKT/AKT was 0.47 ± 0.04 , 1.01 ± 0.08 , 1.26 ± 0.10 , and 0.49 ± 0.04 . The ratio of p-mTOR/mTOR was 0.30 ± 0.02 , 0.62 ± 0.05 , 1.17 ± 0.10 , and 0.30 ± 0.03 , respectively. The ratio of p-HER3/HER3 was 0.67 ± 0.06 , 1.01 ± 0.08 , 1.26 ± 0.10 , and 0.42 ± 0.04 , respectively. As shown in Figure 7B, the expression of GLUT1 and HIF-1 α and the ratio of p-AKT/AKT, p-mTOR/mTOR, and p-HER3/HER3 in each group of the mouse model were detected using western blotting analysis. Respectively, the expression was: GLUT1 0.33 ± 0.03 , 0.80 ± 0.07 , 0.99 ± 0.08 , and 0.48 ± 0.04 ; and HIF-1 α 1.12 ± 0.09 , 0.95 ± 0.08 , 0.73 ± 0.06 , and 1.26 ± 0.10 . Respectively, the ratio of p-AKT/AKT was 0.52 ± 0.04 , 0.91 ± 0.08 , 1.55 ± 0.13 , and 0.95 ± 0.08 . The ratio of p-mTOR/mTOR was 0.71 ± 0.06 , 1.17 ± 0.10 , 1.56 ± 0.13 , and 0.64 ± 0.05 , respectively. The ratio of p-HER3/HER3 was 0.54 ± 0.04 , 1.06 ± 0.09 , 1.08 ± 0.09 , and 0.82 ± 0.07 , respectively.

The results show that the PI3K/mTOR signalling pathway was activated after treatment with tanshinone IIA, and the effect was more significant after overexpression of GLUT1. These results indicate that the effect of increasing the expression of aerobic oxidation of glucose related enzymes might be mediated by the PI3K/AKT/mTOR signalling pathway.

The effect of tanshinone IIA on the expression of neuronal protective factors in the mouse and cell models

As shown in Figure 8, the concentration of neuronal protective factors in the serum samples and cellular medium were detected using ELISA. Respectively, in the serum samples of mice from the NC, TT, TO, and TI groups, the concentration was: neurotrophin-3 241.2 ± 18.6 , 292.3 ± 21.3 , 354.2 ± 27.1 , and 250.7 ± 19.4 pg/ml; calprotectin 806.1 ± 35.2 , 874.5 ± 40.3 , 985.6 ± 47.1 , and 810.2 ± 33.6 pg/ml; GFAP 202.1 ± 16.4 ,

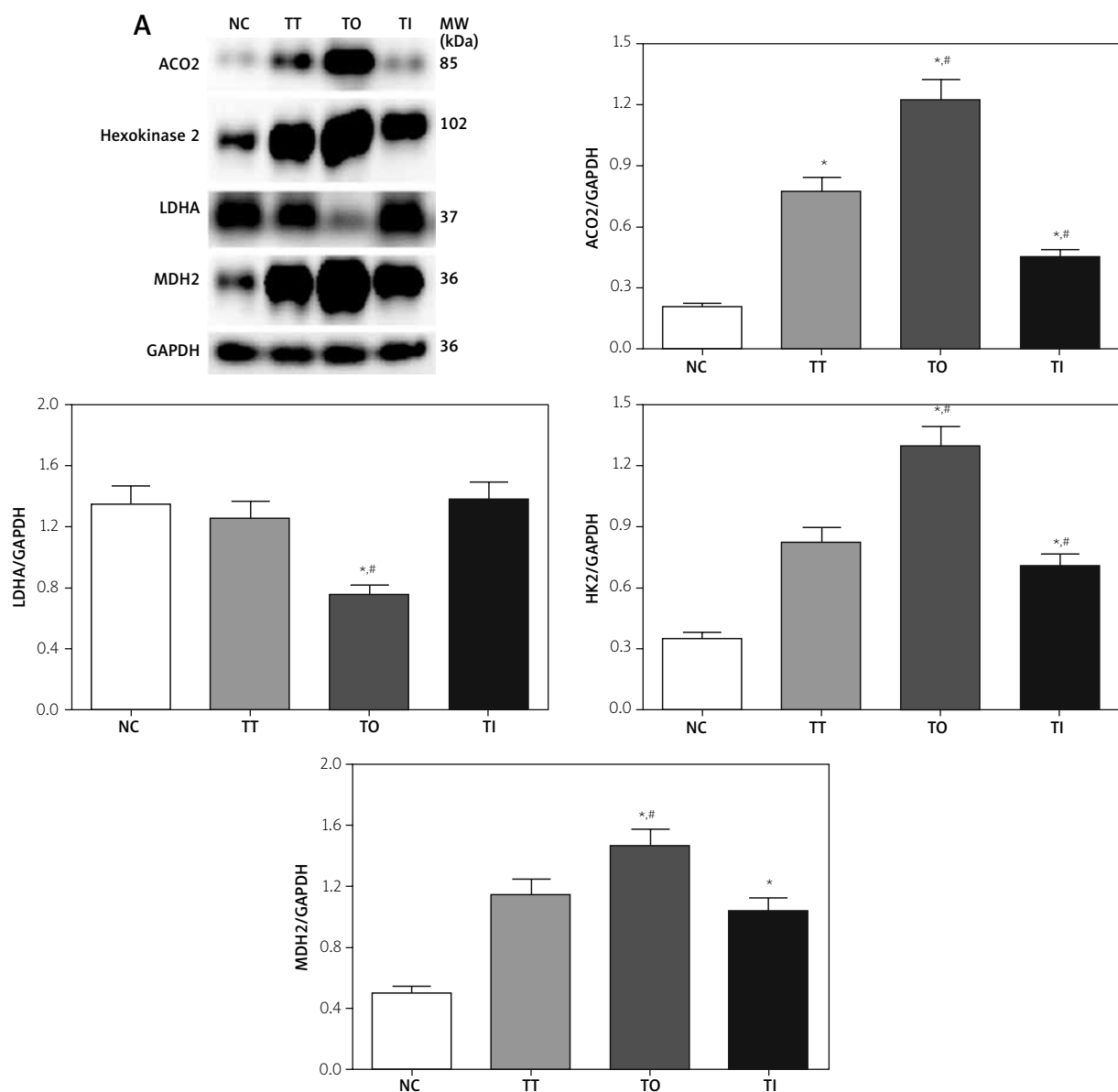


Fig. 6. The expression of ACO2, hexokinase 2, LDHA, and MDH2. **A)** The expression and quantitative analysis of these enzymes in each group of cell model.

245.3 ± 20.6, 321.4 ± 26.6, and 210.5 ± 19.4 pg/ml; and nitric oxide 48.6 ± 9.6, 60.2 ± 12.3, 78.1 ± 14.1, and 52.3 ± 10.7 μmol/l. The respective ratios of GSH/GSSG in these groups were 1.2 ± 0.1, 1.9 ± 0.2, 2.7 ± 0.4, and 1.6 ± 0.1. The respective relative intensity of ROS in the TT, TO, and TI groups was 0.72 ± 0.07, 0.51 ± 0.04, and 0.94 ± 0.08. As shown in Figure 9, the concentration in the culture medium of each respective group of cells was: neurotrophin-3 107.2 ± 13.5, 142.4 ± 16.4, 213.6 ± 19.7, and 116.2 ± 17.7 pg/ml; calprotectin 520.3 ± 23.2, 578.1 ± 26.1, 654.4 ± 33.5, and 540.3 ± 24.5 pg/ml;

GFAP 137.2 ± 13.7, 154.1 ± 17.4, 198.7 ± 20.5, and 145.2 ± 16.2 pg/ml; and nitric oxide 26.5 ± 3.6, 31.2 ± 4.5, 46.3 ± 5.3, and 25.4 ± 4.0 μmol/l. The respective ratios of GSH/GSSG in these groups were 0.8 ± 0.1, 1.1 ± 0.2, 1.8 ± 0.3, and 1.0 ± 0.2, respectively. The respective relative intensity of ROS was 0.81 ± 0.07, 0.60 ± 0.04, and 1.12 ± 0.11.

Discussion

Stroke is one of the major health problems around the world and is the third leading cause of death [11].

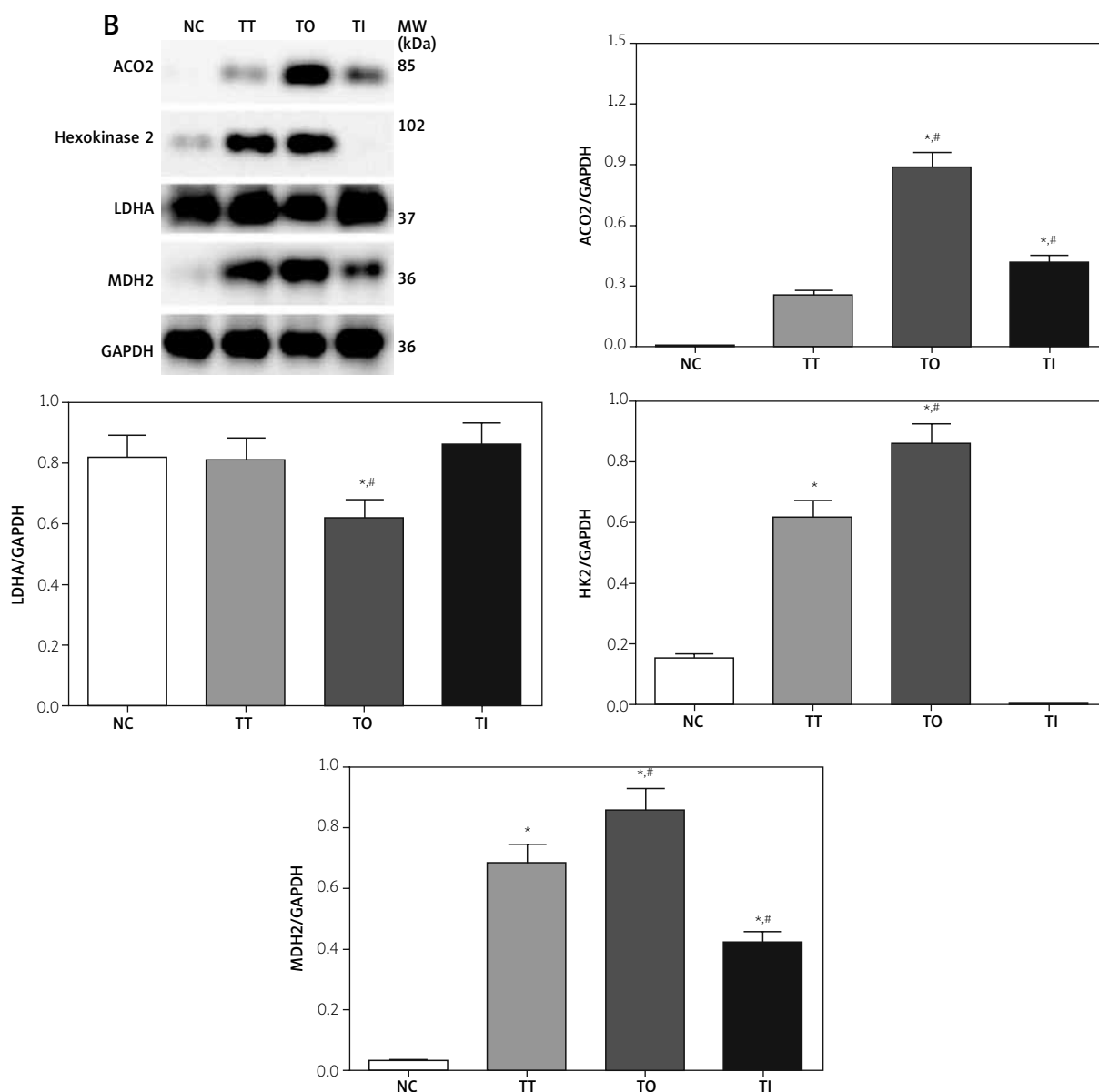


Fig. 6. Cont. The expression of ACO2, hexokinase 2, LDHA, and MDH2. **B)** The expression and quantitative analysis of these enzymes in each group of mouse model. Data presented as mean \pm SD. Each experiment was repeated three times independently. * $p < 0.05$ compared with NC group. # $p < 0.05$ compared with TT group.

Among affected patients, nearly 87% of them suffer an ischaemic stroke caused by interruption of the blood supply to the brain. Tanshinone IIA is a traditional Chinese medicine extracted from the roots of *Salvia miltiorrhiza* (Bunge) and has been widely used in the treatment of cardiovascular and cerebrovascular disorders [34]. Glucose is transported into brain cells *via* members of the GLUT family, including GLUT1 in the endothelium and glial cells and GLUT3 in neurons [4,38]. Under normal and pathological

conditions, the concentration of glucose in neurons is strictly controlled and thus changes in the expression of GLUT1 might severely affect the function of neurons. Thus, we thought overexpression of GLUT1 might be helpful in enhancing the recovery of neurons *via* increasing the flux of glucose [3].

The MTT assay indicated that the viability rate of the cells was increased after tanshinone IIA treatment and was even higher after overexpression of GLUT1. In addition, using *in vivo* experiments, we

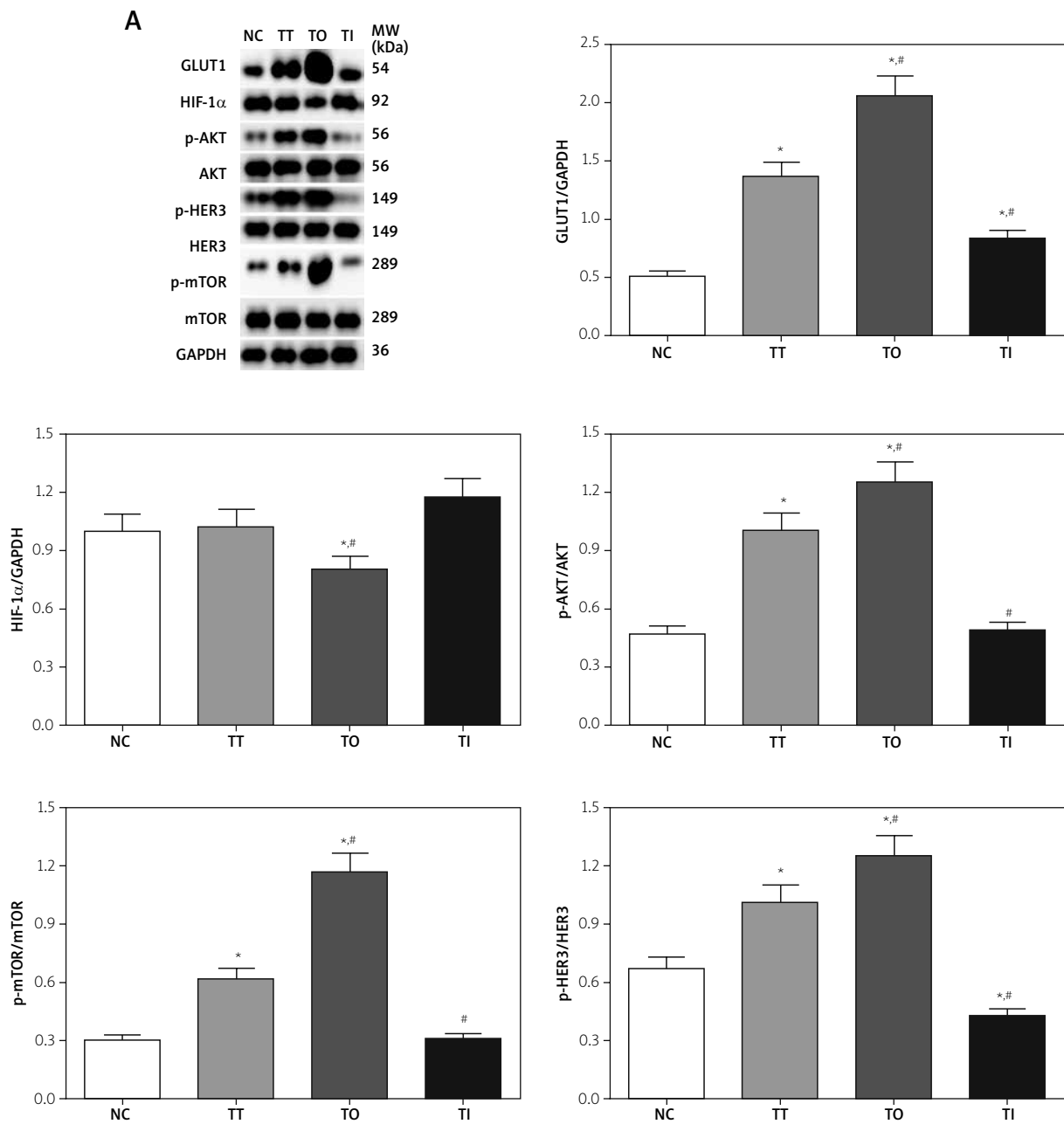


Fig. 7. The activation of PI3K/AKT/mTOR signalling pathway. **A)** The activation and quantitative analysis of PI3K/AKT/mTOR in each group of cell model.

noticed that the time of escape latency, average number of platform crossings, and time in the target quadrant were significantly improved after treatment with tanshinone IIA combined with overexpression of GLUT1. In addition, we also noticed that the concentration of glucose and glucose uptake ability were also increased, indicating that the recovery of cell viability and brain function might

be mediated by increased glucose uptake and energy supplies. However, the detailed mechanism was not clear. A previous study found that tanshinone IIA could delay the development of atherosclerosis *via* inhibition of inflammatory responses [28]. Thus, we also detected the expression of inflammatory response-related genes, including COX-2, IL-1 β , PGE2, and MCP-1.

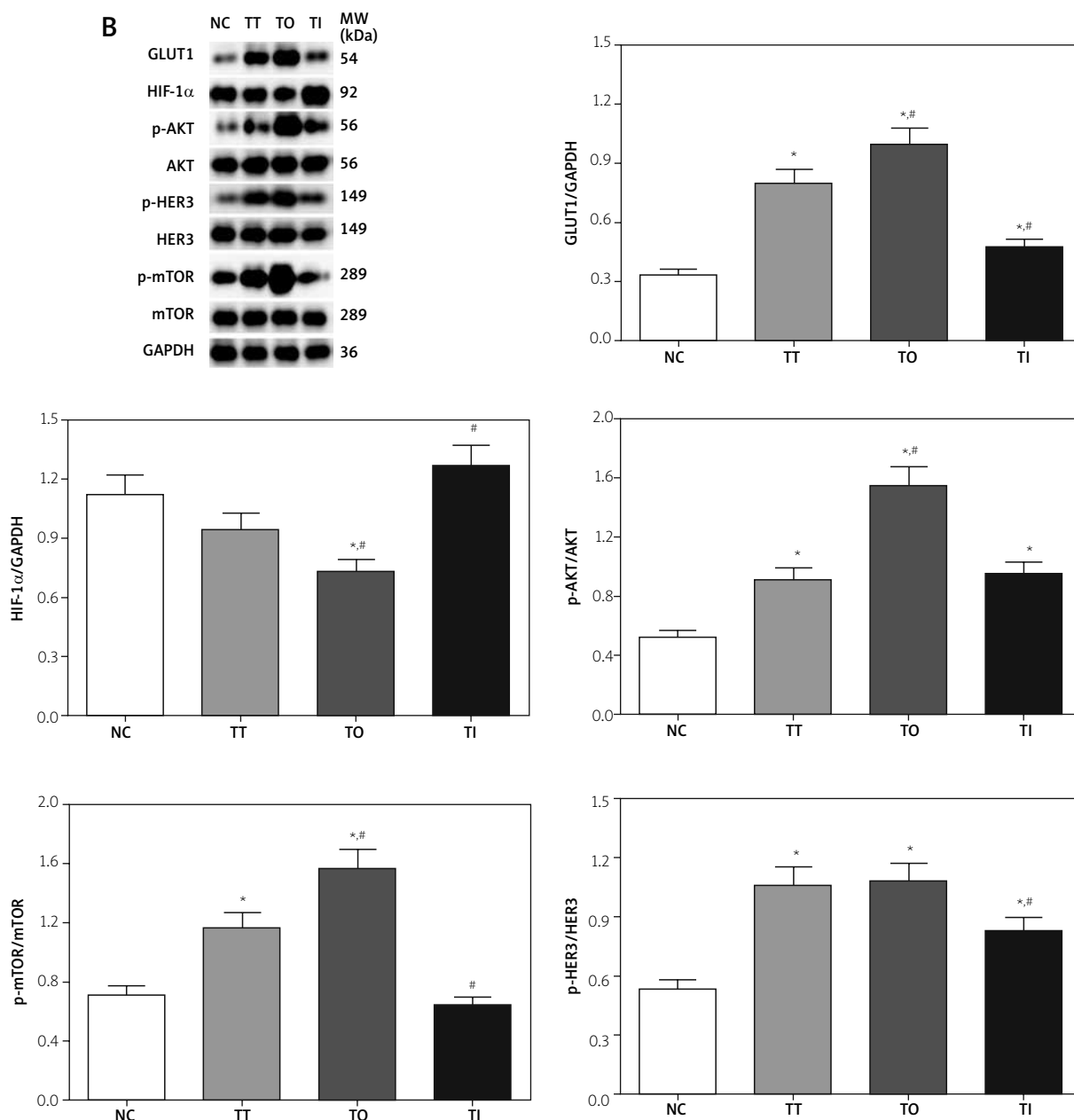


Fig. 7. Cont. The activation of PI3K/AKT/mTOR signalling pathway. **B)** The activation and quantitative analysis of PI3K/AKT/mTOR in each groups of mice model. Data was presented as mean \pm SD. Each experiment was repeated for three times independently. * $p < 0.05$ compared with NC group. # $p < 0.05$ compared with TT group.

Cyclooxygenase enzymes are critical for the synthesis of prostaglandins and participate in the inflammatory response process [24]. A previous study found that COX-2 directly affects the function of the CNS serotonergic system via the inflammatory process, and a higher level of serotonin in the frontal and temporoparietal cortices was observed after administration of rofecoxib, a selective inhibi-

tor of COX-2 [37], restoring the basic function of the CNS system. IL-1 β is one of the most important pro-inflammatory factors, and its expression is generally increased after experimental and human TBI. It is mainly produced by microglia, endothelial cells, and astrocytes [20,22]. High expression of IL-1 β often occurs in the early and delayed phase after TBI in humans [18]. In addition, the production of

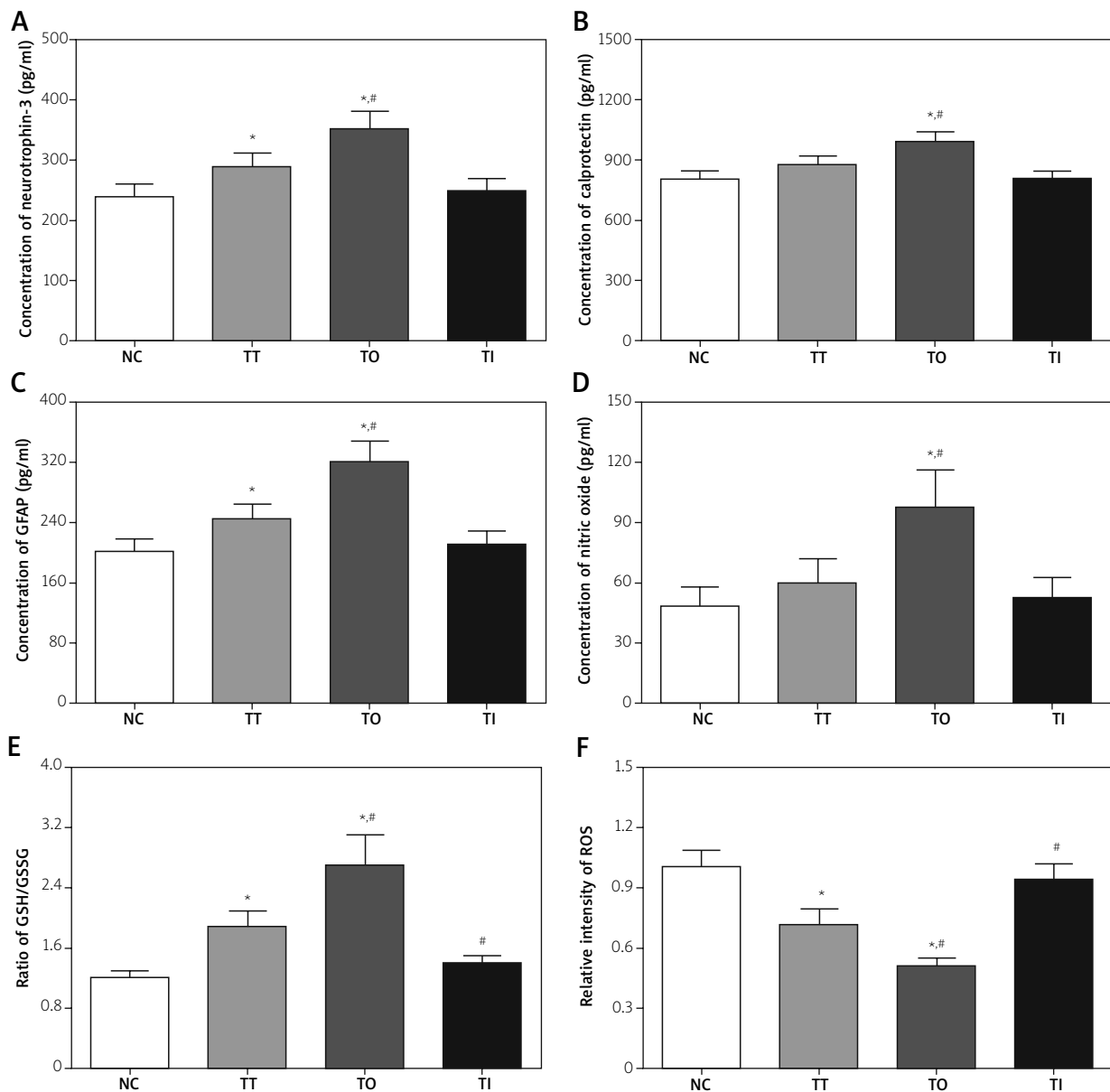


Fig. 8. The concentration of in cultured medium of neurotrophin-3, calprotectin, GFAP, and nitric oxide, and the ratio of GSH/GSSG, relative intensity of ROS of cells. **A)** The concentration of neurotrophin-3 in cultured medium of cells. **B)** The concentration of calprotectin in cultured medium of cells. **C)** The concentration of GFAP in cultured medium of cells. **D)** The concentration of nitric oxide in cultured medium of cells. **E)** The ratio of GSH/GSSG in cultured medium of cells. **F)** The relative intensity of ROS in cultured medium of cells. Data presented as mean \pm SD. Each experiment was repeated three times independently. * $p < 0.05$ compared with NC group. # $p < 0.05$ compared with TT group.

IL-1 β is closely related to the severity of the injury [25]. PGE2 is a subtype of the prostanoid family and presents a wide range of biological effects related to inflammation and cancer. PGE2 can increase the response of neurons to pain and promote a pyrogenic effect in the preoptic area [43]. The role of PGE2

in inflammation has been detected in a number of disease models and could be facilitated by mPGES-1 knockout [41]. The expression of PGE2 is highly regulated by microsomal PGE synthase-1 (mPGES-1), mPGES-2, and cytosolic PGE synthase (cPGES) [21], while the expression of mPGES-1 is expressed in the

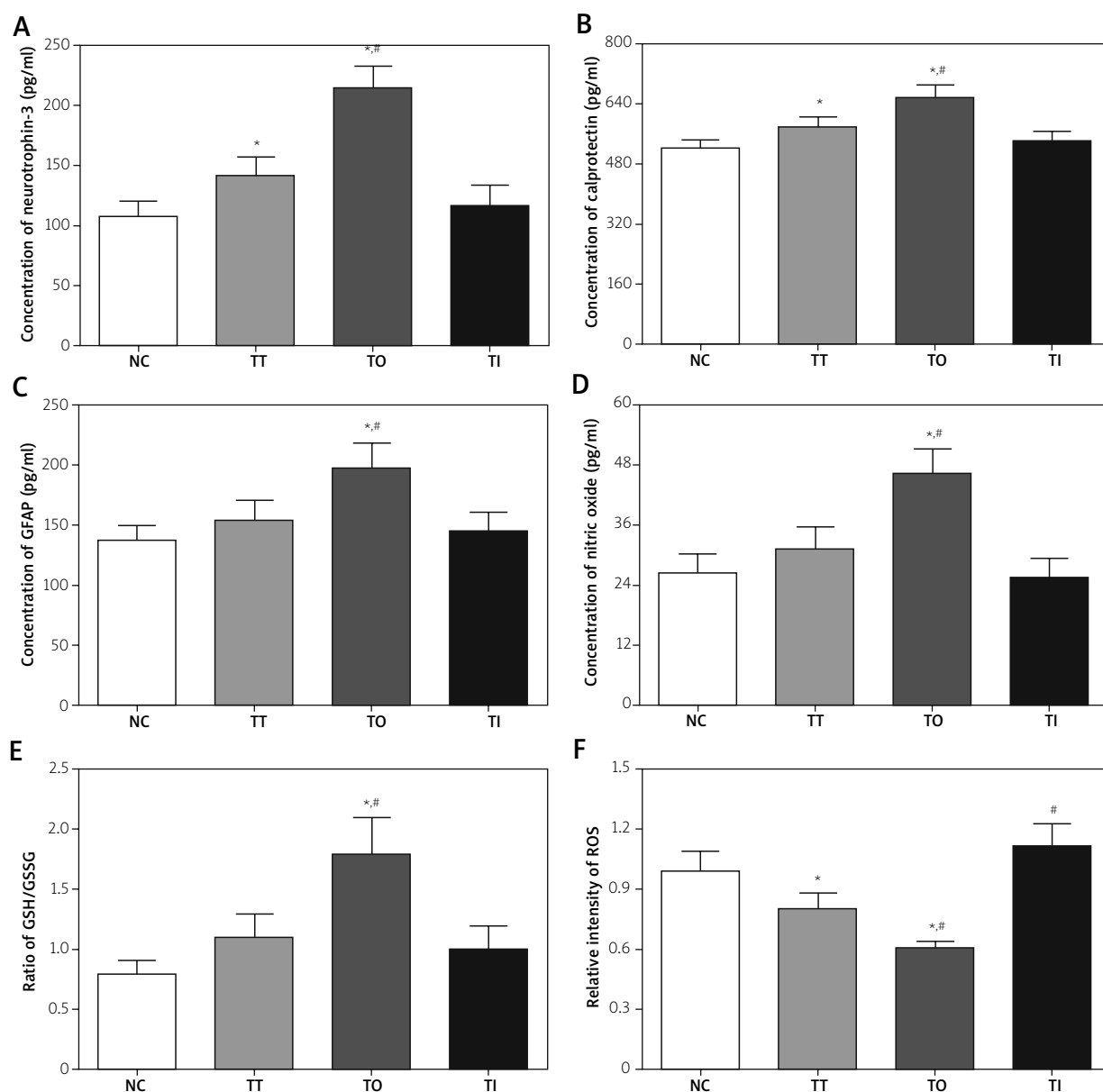


Fig. 9. The concentration of in serum sample of neurotrophin-3, calprotectin, GFAP, nitric oxide, and the ratio of GSH/GSSG, relative intensity of ROS of mouse model. **A)** The concentration of neurotrophin-3 in serum sample of mouse model. **B)** The concentration of calprotectin in serum sample of mouse model. **C)** The concentration of GFAP in serum sample of mouse model. **D)** The concentration of nitric oxide in serum sample of mouse model. **E)** The ratio of GSH/GSSG in serum sample of mouse model. **F)** The relative intensity of ROS in serum sample of mouse model. Data presented as mean ± SD. Each experiment was repeated three times independently. **p* < 0.05 compared with NC group. #*p* < 0.05 compared with TT group.

same pattern as COX-2 under various stimulations, further inducing the expression of PGE2 [31]. Monocyte chemoattractant protein-1 (MCP-1) belongs to the family of CC chemokines and is expressed in glial cells and neurons under normal and inflammatory stimulation [5,6]. In addition to participating in the

attraction of monocytes and macrophages to the site of inflammation, MCP-1 also mediates the transendothelial migration of inflammation cells across the blood-brain barrier into the CNS [17]. The results of our present study indicated that tanshinone IIA treatment decreased the expression of these inflam-

mation-related factors, and overexpression of GLUT1 enhanced this trend. The inhibition of the inflammatory process in neurons was observed in both *in vivo* and *in vitro* experiments.

Aco2, located in the mitochondrial matrix, is an iron-sulphur protein that requires a 4Fe-4S cluster for its enzymatic activity. Its function is to catalyse the conversion of citrate to isocitrate in the tricarboxylic acid (TCA) cycle, an important step involved in ATP generation. Aco2 is susceptible to increased oxidative stress that can inactivate Aco2 activity [40]. Hexokinase2 (HK2) is involved in high-glucose-induced cellular apoptosis and is critical in triggering aerobic glycolysis, further improving cell survival and proliferation [44]. A previous study demonstrated that expression of lactate is increased under oxidative stress along with a reduction of LDHA expression, leading to the consumption of glucose [36], and these processes might be mediated by the MAPK signalling pathway [14]. A recent study also found that overexpression of HK2 might reduce the apoptosis of cells induced by high glucose with a reduction in Bax expression [45]. MDH2 is essential for the conversion of malate to oxaloacetate as part of the proper functioning of the Krebs cycle [7]. MDH2 is activated in the mitochondria, peroxisomes, glyoxysomes, and cytosol, and interacts with the malate-aspartate shuttle (MAS), further contributing to the transfer of reducing equivalents from the cytosol into the mitochondria for oxidation [15]. The present study found that the TCA cycle was activated after treatment with tanshinone IIA, and this trend was increased after overexpression of GLUT1, indicating that overexpression of GLUT1 might contribute to the recovery effect of tanshinone IIA *via* enhancement of the energy supply in neurons.

The PI3K/AKT signalling pathway regulates the cellular activation, inflammatory response, and apoptosis [19], and plays an important role in protection against I/R injury. Activation of AKT contributes to the reduction of infarction and dysfunction after I/R injury [33]. mTOR is a downstream molecule in the PI3K/AKT signalling pathway, and a previous study also found that activation of mTOR contributes to protection against I/R injury [12]. Using an *in vitro* model, researchers found that overexpression of mTOR inhibits the inflammatory response after I/R [2]. A previous study found that ERBB3 (HER3) was mainly localised in the outer areas of T-tubules [8]; however, the function of ERBB3 is not fully under-

stood. A recent study found that the neuregulin receptor degradation protein-1 (Nrdp1), an E3 ligase that targets ERBB3 [10], is upregulated after I/R injury. Using a mouse model, researchers found that mice with overexpression of NRDP1 had a higher infarct size and increases in inflammatory cells [47].

Here, we noticed that overexpression of GLUT1 might enhance the effect of tanshinone IIA in the treatment of cerebral ischaemia-reperfusion through increasing the glucose uptake ability and cellular glucose concentration, along with a reduction in inflammatory response-related factors. We further noticed that these effects might be mediated by activation of the PI3K/mTOR/HER3 signalling pathway.

Disclosure

The authors report no conflict of interest.

References

1. Ashafaq M, Khan MM, Shadab Raza S, Ahmad A, Khuwaja G, Javed H, Khan A, Islam F, Siddiqui MS, Safhi MM, Islam F. S-allyl cysteine mitigates oxidative damage and improves neurologic deficit in a rat model of focal cerebral ischemia. *Nutr Res* 2012; 32: 133-143.
2. Aoyagi T, Kusakari Y, Xiao CY, Inouye BT, Takahashi M, Scherrer-Crosbie M, Rosenzweig A, Hara K, Matsui T. Cardiac mTOR protects the heart against ischemia-reperfusion injury. *Am J Physiol Heart Circ Physiol* 2012; 303: H75-85.
3. Barros LF, San Martín A, Ruminot I, Sandoval PY, Fernández-Moncada I, Baeza-Lehnert F, Arce-Molina R, Contreras-Baeza Y, Cortés-Molina F, Galaz A, Alegría K. Near-critical GLUT1 and Neurodegeneration. *J Neurosci Res* 2017; 95: 2267-2274.
4. Barros LF, Bittner CX, Loaiza A, Porras OH. A quantitative overview of glucose dynamics in the gliovascular unit. *Glia* 2007; 55: 1222-1237.
5. Banisadr G, Gosselin RD, Mechighel P, Kitabgi P, Rostène W, Parsadaniantz SM. Highly regionalized neuronal expression of monocyte chemoattractant protein-1 (MCP-1/CCL2) in rat brain: evidence for its colocalization with neurotransmitters and neuropeptides. *J Comp Neurol* 2005; 489: 275-292.
6. Berman JW, Guida MP, Warren J, Amat J, Brosnan CF. Localization of monocyte chemoattractant peptide-1 expression in the central nervous system in experimental autoimmune encephalomyelitis and trauma in the rat. *J Immunol* 1996; 156: 3017-3023.
7. Cascón A, Comino-Méndez I, Currás-Freixes M, de Cubas AA, Contreras L, Richter S, Peitzsch M, Mancikova V, Inglada-Pérez L, Pérez-Barrios A, Calatayud M, Azriel S, Villar-Vicente R, Aller J, Setién F, Moran S, Garcia JF, Río-Machín A, Letón R, Gómez-Graña Á, Apellániz-Ruiz M, Roncador G, Esteller M, Rodríguez-Antona C, Satrustegui J, Eisenhofer G, Urioste M, Robledo M. Whole-exome sequencing identifies MDH2 as a new familial paraganglioma gene. *J Natl Cancer Inst* 2015; 107: djv053.

8. Campreciós G, Lorita J, Pardina E, Peinado-Onsurbe J, Soley M, Ramírez I. Expression, localization, and regulation of the neuregulin receptor ErbB3 in mouse heart. *J Cell Physiol* 2011; 226: 450-455.
9. Chen FY, Guo R, Zhang BK. Advances in cardiovascular effects of tanshinone II (A). *Zhongguo Zhong Yao Za Zhi* 2015; 40: 1649-1653.
10. Diamonti AJ, Guy PM, Ivanof C, Wong K, Sweeney C, Carraway KL 3rd. An RBCC protein implicated in maintenance of steady-state neuregulin receptor levels. *Proc Natl Acad Sci U S A* 2002; 99: 2866-2871.
11. Feher A, Pusch G, Koltai K, Tibold A, Gasztonyi B, Szapary L, Feher G. Statintherapy in the primary and the secondary prevention of ischaemic cerebrovascular diseases. *Int J Cardiol* 2011; 148: 131-138.
12. Fuglesteig BN, Tiron C, Jonassen AK, Mjøs OD, Ytrehus K. Pre-treatment with insulin before ischaemia reduces infarct size in Langendorff-perfused rat hearts. *Acta Physiol (Oxf)* 2009; 195: 273-282.
13. Gao S, Liu Z, Li H, Little PJ, Liu P, Xu S. Cardiovascular actions and therapeutic potential of tanshinone IIA. *Atherosclerosis* 2012; 220: 3-10.
14. Galardo MN, Regueira M, Riera MF, Pellizzari EH, Cigorraga SB, Meroni SB. Lactate regulates rat male germ cell function-through reactive oxygen species. *PLoS One* 2014; 9: e88024.
15. Gietl C. Malate dehydrogenase isoenzymes: cellular locations and role in the flow of metabolites between the cytoplasm and cell organelles. *Biochim Biophys Acta* 1992; 1100: 217-234.
16. Gresita A, Glavan D, Udristoiu I, Catalin B, Hermann DM, Popa-Wagner A. Very low efficiency of direct reprogramming of astrocytes into neurons in the brains of young and aged mice after cerebral ischemia. *Front Aging Neurosci* 2019; 11: 334.
17. Hayashi M, Luo Y, Laning J, Strieter RM, Dorf ME. Production and function of monocyte chemoattractant protein-1 and other β -chemokines in murine glial cells. *J Neuroimmunol* 1995; 60: 143-150.
18. Holmin S, Höjeberg B. In situ detection of intracerebral cytokine expression after human brain contusion. *Neurosci Lett* 2004; 369: 108-114.
19. Hu X, Xu C, Zhou X, Cui B, Lu Z, Jiang H. PI3K/Akt signaling pathway involved in cardioprotection of preconditioning with high mobility group box 1 protein during myocardial ischemia and reperfusion. *Int J Cardiol* 2011; 150: 222-223.
20. Hutchinson PJ, O'Connell MT, Rothwell NJ, Hopkins SJ, Nortje J, Carpenter KL, Timofeev I, Al-Rawi PG, Menon DK, Pickard JD. Inflammation in human brain injury: Intracerebral concentrations of IL-1 α , IL-1 β , and their endogenous inhibitor IL-1ra. *J Neurotrauma* 2007; 24: 1545-1557.
21. Jakobsson PJ, Thoren S, Morgenstern R, Samuelsson B. Identification of human prostaglandin E synthase: a microsomal, glutathione-dependent, inducible enzyme, constituting a potential novel drug target. *Proc Natl Acad Sci U S A* 1999; 96: 7220-7225.
22. Kamm K, Vanderkolk W, Lawrence C, Jonker M, Davis AT. The effect of traumatic brain injury upon the concentration and expression of interleukin-1 β and interleukin-10 in the rat. *J Trauma* 2006; 60: 152-157.
23. Kayano T, Fukumoto H, Eddy RL, Fan YS, Byers MG, Shows TB, Bell GI. Evidence for a family of human glucose transporter-like proteins. Sequence and gene localization of a protein expressed in fetal skeletal muscle and other tissues. *J Biol Chem* 1988; 263: 15245-15248.
24. Kessing LV, Rytgaard HC, Gerds TA, Berk M, Ekstrom CT, Andersen PK. New drug candidates for depression – a nationwide population-based study. *Acta Psychiatr Scand* 2019; 139: 68-77.
25. Kinoshita K, Chatzipanteli iK, Vitarbo E, Truettner JS, Alonso OF, Dietrich WD. Interleukin-1 β messenger ribonucleic acid and protein levels after fluid-percussion brain injury in rats: Importance of injury severity and brain temperature. *Neurosurgery* 2002; 51: 195-203.
26. Lee M, Saver JL, Hong KS, Wu YL, Liu HC, Rao NM, Ovbiagele B. Cognitive impairment and risk of future stroke: a systematic review and meta-analysis. *CMAJ* 2014; 186: E536-546.
27. Leino RL, Gerhart DZ, van Bueren AM, McCall AL, Drewes LR. Ultrastructural localization of GLUT 1 and GLUT 3 glucose transporters in rat brain. *J Neurosci Res* 1997; 49: 617-626.
28. Li Y, Guo Y, Chen Y, Wang Y, You Y, Yang Q, Weng X, Li Q, Zhu X, Zhou B, Liu X, Gong Z, Zhang R. Establishment of an interleukin-1 β -induced inflammation-activated endothelial cell-smooth muscle cell-mononuclear cell co-culture model and evaluation of the anti-inflammatory effects of tanshinone IIA on atherosclerosis. *Mol Med Rep* 2015; 12: 1665-1676.
29. Livak KJ, Schmittgen TD. Analysis of relative gene expression data using real-time quantitative PCR and the 2(-Delta Delta C(T)) method. *Methods* 2001; 25: 402-408.
30. Maher F. Immunolocalization of GLUT1 and GLUT3 glucose transporters in primary cultured neurons and glia. *J Neurosci Res* 1995; 42: 459-469.
31. Murakami M, Naraba H, Tanioka T, Semmyo N, Nakatani Y, Kojima F, Ikeda T, Fueki M, Ueno A, Oh S, Kudo I. Regulation of prostaglandin E2 biosynthesis by inducible membrane-associated prostaglandin E2 synthase that acts in concert with cyclooxygenase-2. *J Biol Chem* 2000; 275: 32783-32792.
32. Nagamatsu S, Kornhauser JM, Burant CF, Seino S, Mayo KE, Bell GI. Glucose transporter expression in brain. cDNA sequence of mouse GLUT1, the brain facilitative glucose transporter isoform, and identification of sites of expression by in situ hybridization. *J Biol Chem* 1992; 267: 467-472.
33. Nagoshi T, Matsui T, Aoyama T, Leri A, Anversa P, Li L, Ogawa W, del Monte F, Gwathmey JK, Grazette L, Hemmings BA, Kass DA, Champion HC, Rosenzweig A. PI3K rescues the detrimental effects of chronic Akt activation in the heart during ischemia/reperfusion injury. *J Clin Invest* 2005; 115: 2128-2138.
34. Park YK, Obiang-Obounou BW, Lee J, Lee TY, Bae MA, Hwang KS, Lee KB, Choi JS, Jang BC. Anti-adipogenic effects on 3T3-L1 cells and zebrafish by tanshinone IIA. *Int J Mol Sci* 2017; 18, pii: E2065.
35. Pendlebury ST, Rothwell PM. Prevalence, incidence, and factors associated with pre-stroke and post-stroke dementia: a systematic review and meta-analysis. *Lancet Neurol* 2009; 8: 1006-1018.
36. Potthoff MJ, Inagaki T, Satapati S, Ding X, He T, Goetz R, Mohammedi M, Finck BN, Mangelsdorf DJ, Kliewer SA, Burgess SC. FGF21 induces PGC-1 α and regulates carbohydrate and

- fatty acid metabolism during the adaptive starvation response. *Proc Natl Acad Sci U S A* 2009; 106: 10853-10858.
37. Sandrini M, Vitale G, Pini LA. Effect of rofecoxib on nociception and the serotonin system in the rat brain. *Inflamm Res* 2002; 51: 154-159.
 38. Simpson IA, Carruthers A, Vannucci SJ. Supply and demand in cerebral energy metabolism: the role of nutrient transporters. *J Cereb Blood Flow Metab* 2007; 27: 1766-1791.
 39. Su J, Liu J, Yan XY, Zhang Y, Zhang JJ, Zhang LC, Sun LK. Cytoprotective effect of the UCP2-SIRT3 signaling pathway by decreasing mitochondrial oxidative stress on cerebral ischemia-reperfusion injury. *Int J Mol Sci* 2017; 18: E1599.
 40. Tabrizi SJ, Cleeter MW, Xuereb J, Taanman JW, Cooper JM, Schapira AH. Biochemical abnormalities and excitotoxicity in Huntington's disease brain. *Ann Neurol* 1999; 45: 25-32.
 41. Uematsu S, Matsumoto M, Takeda K, Akira S. Lipopolysaccharide-dependent prostaglandin E(2) production is regulated by the glutathione-dependent prostaglandin E(2) synthase gene induced by the Toll-like receptor 4/MyD88/NF-IL6 pathway. *J Immunol* 2002; 168: 5811-5816.
 42. Vorhees CV, Williams MT. Morris water maze: procedures for assessing spatial and related forms of learning and memory. *Nat Protoc* 2006; 1: 848-858.
 43. Wallace JL. Prostaglandin biology in inflammatory bowel disease. *Gastroenterol Clin North Am* 2001; 30: 971-980.
 44. Wolf A, Agnihotri S, Micallef J, Mukherjee J, Sabha N, Cairns R, Hawkins C, Guha A. Hexokinase 2 is a key mediator of aerobic glycolysis and promotes tumor growth in human glioblastoma multiforme. *J Exp Med* 2011; 208: 313-326.
 45. Zhang J, Guo Y, Ge W, Zhou X, Pan M. High glucose induces apoptosis of HUVECs in a mitochondria-dependent manner by suppressing hexokinase 2 expression. *Exp Ther Med* 2019; 18: 621-629.
 46. Zhang Y, Li C, Meng H, Guo D, Zhang Q, Lu W, Wang Q, Wang Y, Tu P. BYD ameliorates oxidative stress-induced myocardial apoptosis in heart failure post-acute myocardial infarction via the P38 MAPK-CRYAB signaling pathway. *Front Physiol* 2018; 9: 505.
 47. Zhang Y, Zeng Y, Wang M, Tian C, Ma X, Chen H, Fang Q, Jia L, Du J, Li H. Cardiac-specific overexpression of E3 ligase Nrdp1 increases ischemia and reperfusion-induced cardiac injury. *Basic Res Cardiol* 2011; 106: 371-383.
 48. Zhu S, Li W, Liu J, Chen CH, Liao Q, Xu P, Xu H, Xiao T, Cao Z, Peng J, Yuan P, Brown M, Liu XS, Wei W. Genome-scale deletion screening of human long non-coding RNAs using a paired-guide RNA CRISPR-Cas9 library. *Nat Biotechnol* 2016; 34: 1279-1286.